

## Electrochemical Preparation and Characterization of Gold and Platinum Nanoparticles Modified Poly(taurine) Film Electrode and Its Application to Hydrazine Determination

Çağrı Ceylan Koçak<sup>1,\*</sup>, Aylin Altın<sup>2</sup>, Burak Aşlışen<sup>2</sup>, Süleyman Koçak<sup>2</sup>

<sup>1</sup> Bergama Vocational School, Dokuz Eylül University, 35700, İzmir, Turkey.

<sup>2</sup> Department of Chemistry, Faculty of Science & Art, Celal Bayar University, Muradiye Campus, 45140, Manisa, Turkey.

\*E-mail: [ceylan.kocak@deu.edu.tr](mailto:ceylan.kocak@deu.edu.tr)

Received: 28 October 2015 / Accepted: 19 November 2015 / Published: 1 December 2015

---

A highly sensitive hydrazine sensor has been developed by using gold and platinum nanoparticles (NPs) decorated poly(taurine) on modified glassy carbon electrode (GCE). First, poly(taurine) modified glassy carbon electrode was prepared by electropolymerization method using cyclic voltammetry. Then, a thin layer of poly(taurine) is coated electrochemically on a GCE and the effective parameters have been optimized. After taurine polymerization, metal nanoparticles (Au and Pt) were doped by electrochemical reduction from metal ions solution on poly(taurine)/GCE surface. Modified electrodes were characterized by using different surface techniques. The obtaining results were compared with bare GCE, poly(taurine) modified glassy carbon electrode, AuNPs/poly(taurine)/GCE, and PtNPs/poly(taurine)/GCE. The peak potential of hydrazine oxidation on bare GCE, poly(taurine)/GCE, AuNPs/poly(taurine)/GCE, and PtNPs/poly(taurine)/GCE were observed at 690 mV, 401 mV, 341 mV, and -370 mV, respectively. Finally, these modified electrodes were successfully used for the oxidation of hydrazine and exhibited excellent electrocatalytic activity with respect to hydrazine oxidation. The better sensitivity and selectivity exhibited the amperometric techniques to compare other techniques. The linear concentration ranges were found between 0.1 to 1000  $\mu\text{M}$  ( $R^2 = 0.9981$ ) for AuNPs/poly(taurine)/GCE. The limit of detection (LOD) and limit of quantitation (LOQ) values were calculated to be 0.05  $\mu\text{M}$  and 0.15  $\mu\text{M}$ , respectively. The practical application of the sensor was evaluated in river water samples with good recoveries.

---

**Keywords:** poly(taurine), hydrazine, gold nanoparticles, platinum nanoparticles.

### 1. INTRODUCTION

Hydrazine is widely used in agriculture and industrial applications as air bags, rocket fuel, fuel cells, inhibitor, etc [1]. Also, it has been recognized as a carcinogenic substance by Environmental

Protection Agency (EPA) [2]. There are different reported techniques for the determination of hydrazine, such as spectrophotometry [3], amperometry [4], linear sweep voltammetry [5], titrimetry [6], chemiluminescence [7], flow injection analysis [8], and ion chromatography [9]. Electrochemical techniques [10] can be employed for the direct determination, but hydrazine electro-oxidation is kinetically slow and requires a high overpotential with conventional electrodes. Chemically modified electrodes with an immobilized electrocatalyst have been used to decrease this overpotential [11, 12]. Among diverse methods that have been reported for the determination of hydrazine, voltammetric methods have many advantages such as good selectivity, high sensitivity, rapid response, wide linear range, and simple operating procedures [13–15].

Amino acids are essential components of peptides and for all organisms. Also, they have been in the structure different functional groups such as  $-\text{COOH}$ ,  $-\text{OH}$ ,  $-\text{NH}_2$ ,  $-\text{CH}_x$ , etc. Amino acids can be polymerized with their functional groups in the side chain. Taurine ( $\text{C}_2\text{H}_7\text{NO}_3\text{S}$ ) is a derivative of cysteine, an amino acid which contains a thiol group. It has many fundamental biological roles such as conjugation of acids, antioxidation, membrane stabilization, and modulation of calcium signaling. It is essential for cardiovascular function, development, function of skeletal muscle, the retina, and the central nervous system. It has been commonly used as a food nutrition enhancer and a common drug [16].

There are only a few reports about poly(taurine) modified electrode surface such as poly(taurine)/GCE for the simultaneous determination of epinephrine and dopamine [16], poly(taurine)/MWNT for the detection of acetaminophen [17], poly(taurine)/ $\text{TiO}_2$ -graphene composite film for acetaminophen and caffeine [18], poly(taurine)/zirconia nanoparticles for detection of ractopamine and salbutamol in pig meat, and human urine samples [19]. However, there was no data on the hydrazine oxidation Au and Pt nanoparticles modified poly(taurine)/GCE under neutral conditions.

The applications of nanoparticles in electrochemical sensors have their unique capabilities to change mass transport, facilitate catalysis, and increase surface area [20]. Moreover, the nanoparticles provide a large specific surface area and mass transport enhancement [21]. The catalytic properties of metal particles severely depend on the shape and size [22]. In the last years, the conducting polymer-based nanoparticles composite materials showed high electro-catalytic activity and resulted in the development of electrochemical techniques for their preparation [23]. Gold [5, 24–28], silver [29], palladium [30–32], and platinum [27, 33, 34] nanoparticles have been commonly employed in many electrochemical fields because of their advantages of catalysis, the high effective surface area, and the mass transport.

In this study, an electropolymerized film of taurine was prepared on the surface of glassy carbon electrode (GCE) by cyclic voltammetry for the determination of hydrazine. Furthermore, Au and Pt nanoparticles were doped on the poly(taurine)/GCE. AuNPs/poly(taurine)/GC and PtNPs/poly(taurine)/GC electrodes were synthesized by a simple process and their electro-catalytic behaviors towards hydrazine oxidation evaluated by cyclic voltammetry. These electrodes were characterized by using SEM-EDX, AFM, and XRD. The prepared modified electrodes showed good sensitivity, selectivity, and reproducibility, these electrodes were low in cost and they were used on a

renewable surface. Additionally, conductivities of these modified electrodes were investigated by electrochemical impedance spectroscopy (EIS).

## 2. EXPERIMENTAL

### 2.1. Apparatus

Cyclic voltammetry and EIS were performed on an Autolab potentiostat-galvanostat (PGSTAT 101 and PGSTAT 128N) with a three electrode system. A conventional three-electrode electrochemical system was used for all electrochemical experiments, which consisted of a working electrode (having a 3 mm diameter glassy carbon electrode), auxiliary electrode (a bright platinum wire), and a reference electrode (Ag/AgCl (sat. KCl)). For AFM analysis, an indium tin oxide (ITO) on a thin film coated glass was used.

The surface characterizations were examined by using SEM (FEI QUANTA 250FEG), AFM (Digital Instruments-MMSPM Nanoscope IV), and XRD (PANalytical Empyrean). Ultra-pure water (18.1 Mohm purity) and MilliQ Ultra-High Water (MILLIPORE) was used.

### 2.2. Chemicals

All reagents were of analytical grade and were used as received. Hydrazine ( $\text{N}_2\text{H}_4 \cdot \text{H}_2\text{SO}_4$ ) was obtained from Merck. Taurine ( $\text{C}_2\text{H}_7\text{NO}_3\text{S}$ ) was obtained from Alfa Aesar. All solutions were prepared with ultra-pure water. The solutions of taurine and hydrazine were prepared at prior for measurements. Au wire (diam.1mm, 99.999% in purity) was purchased from Sigma Aldrich. 1.0 mM  $\text{HAuCl}_4$  was prepared by diluting the concentrated  $\text{Au}^{3+}$  solution with 0.1 M HCl after dissolving the Au wire in  $\text{HNO}_3:\text{HCl}$  (1:3). Hexachloroplatinic (IV) acid ( $\text{H}_2\text{PtCl}_6$ ) was purchased from Merck. Phosphate buffer solution (PBS) was prepared with 0.1 M  $\text{H}_3\text{PO}_4$  and pH was adjusted with 3 M NaOH. Glassy carbon electrode was prepared by polishing alumina in ultra pure water with a polishing cloth and finally, sonicated in ultra-pure water for five minutes. All of the experiments were carried out at room temperature of  $25 \pm 2$  °C.

### 2.3. Preparation of the Taurine polymer film modified GCE and ITO

The poly(taurine) film modified electrode was prepared by electrochemical polymerization of taurine on a glassy carbon electrode and an ITO in 2 mM taurine containing pH 7.0 phosphate buffer solution with cyclic voltammetry in the potential range between -1.5 V to 2.0 V at the scan rate of 50  $\text{mV s}^{-1}$ . After 10 cycles, the surface of the electrode was washed with ultra pure water to remove the physically adsorbed materials.

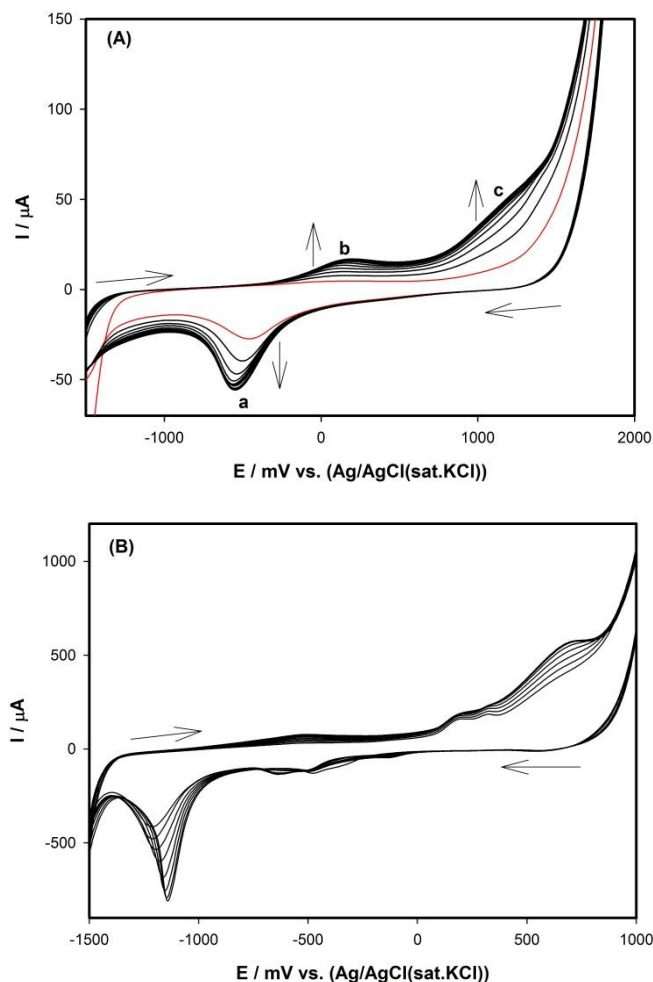
## 2.4. Real sample analysis

Gediz River water samples were collected from the Gediz River near an organized industrial zone in Manisa (Turkey). The AuNPs/poly(aurine)/GC electrode was applied to determination of hydrazine in river water. The Gediz River samples were filtered through 0.45 mm pore size Minisart ny25 syringe membrane filters and stored at 4°C in polyethylene bottles. The sample was analyzed by amperometry. For the analysis, 3.0 mL of the river water was diluted to 10 mL with pH 7.0 PBS.

## 3. RESULTS AND DISCUSSION

### 3.1. Electropolymerization of Taurine and formation of metal nanoparticle on poly(aurine) film

The cyclic voltammogram of 2 mM taurine in pH 7.0 PBS at bare glassy carbon electrode is shown in Figure 1A. During the polymerization process, a cathodic peak at about -500 mV (peak a) and anodic peak at about +100 mV (peak b) and about + 1120 mV (peak c) were observed due to the formation of poly(aurine). After the 2<sup>nd</sup> scan, the current of peak (a), (b), and (c) were increased with an increasing scan number [17, 18]. The current response was the maximum number up to scan number 10 and it decreased thereafter. Therefore, 10 cycles as optimum cycle numbers were chosen.



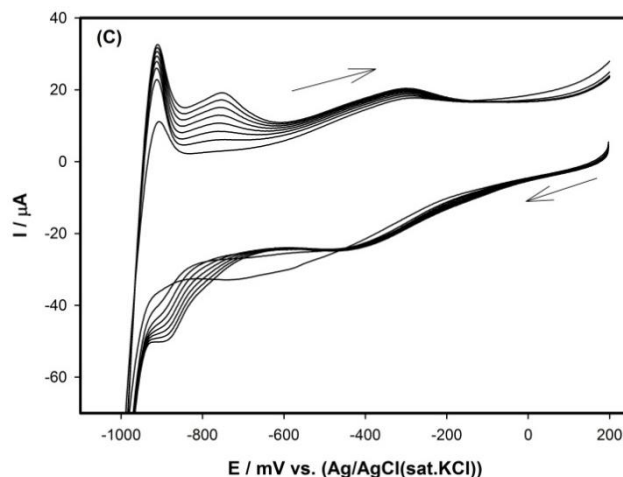


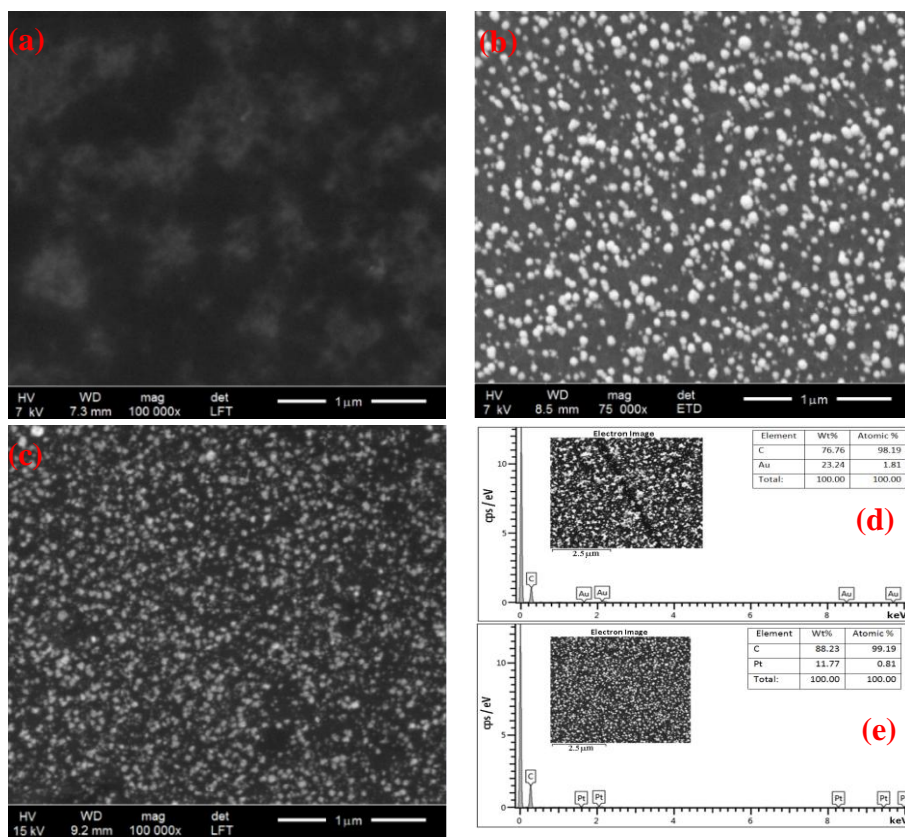
**Figure 1.** Cyclic voltammograms of (A) taurine in polymerization process from 1 to 10 cycles for 2.0 mM taurine in pH 7.0 PBS, and Repetitive cyclic voltammograms recorded at 1.0 mM (B)  $\text{HAuCl}_4$  solution and (C)  $\text{H}_2\text{PtCl}_6$  solution,  $100 \text{ mVs}^{-1}$ .

The electrochemical deposition of Au and Pt nanoparticles were performed using the electrochemical reduction of 1 mM  $\text{HAuCl}_4$  [5] and  $\text{H}_2\text{PtCl}_6$  solution on the poly(taurine)/GCE in 0.1 M HCl solution. Figure 1B and C show the formation of Au and Pt nanoparticles on the poly(taurine)/GCE that was carried out by cyclic voltammetry at a scan rate of  $100 \text{ mVs}^{-1}$  for eight cycles. During the electrodeposition process, the size and amount of the deposited Au and Pt nanoparticles can be controlled. The amount of the nanoparticles deposited on the electrode surface was very important on the catalytic efficiency. Therefore, 8 optimum number of cycles were chosen in the depositing (Au and Pt).

### 3.2. Surface Characterization of modified GCE and ITO

Au and Pt nanoparticles on the poly(taurine)/GCE surface were characterized by the SEM. Figure 2 shows SEM images of bare GCE, poly(taurine)/GCE, and AuNPs/poly(taurine)/GCE films consisting of gold nanoparticles and PtNPs/poly(taurine)/GCE films consisting of platinum nanoparticles. The formation of poly(taurine) was displayed with homogeneously covered on the surface of GCE (Figure 2a). The size of AuNPs was found to be between 20 and 120 nm (Figure 2b). It was obviously clear that AuNPs were deposited on the surface of poly(taurine)/GCE and resulted in spherical geometry decorated nano-agglomerates that homogeneously covered on a significant portion of the poly(taurine)/GCE [5]. Also, it was observed that PtNPs were homogeneously dispersed on the poly(taurine) by excellent adhesion and the strong interfacial bonds.

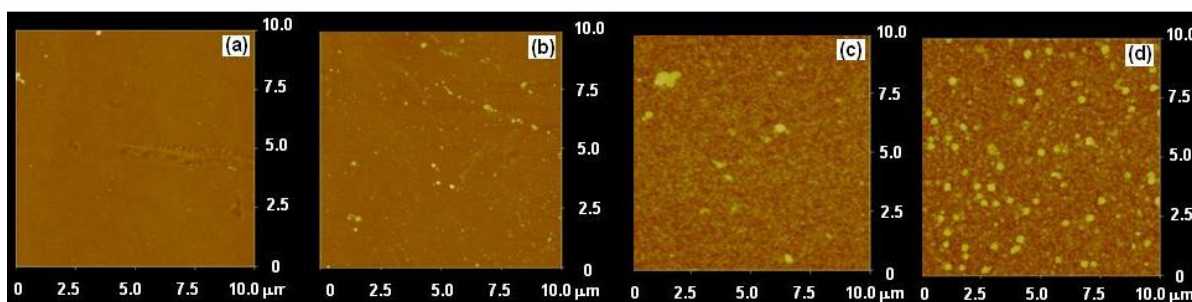
SEM image of PtNPs gave us information about nanoparticle diameter that was in the range from 10 up to 70 nm (Figure 2c). On the other hand, the diameter of AuNPs on poly(taurine)/GCE was much larger than that of the Pt on poly(taurine)/GCE. Thus, poly(taurine) film was a good host material for dispersing Au and Pt nanoparticles. These SEM images of nanoparticles agreed substantially with previous studies [27, 35].



**Figure 2.** SEM image of (a) poly(taurine)/GCE, (b) AuNPs/poly(taurine)/GCE, (c) PtNPs/poly(taurine)/GCE, and EDX spectra for (d) AuNPs/poly(taurine)/GCE, (e) PtNPs/poly(taurine)/GCE.

This was very important in improving the catalytic activity and durability of the catalyst. Energy-dispersive X-ray analysis (EDX) was used to analyze the elemental content of modified electrodes. The weight ratios of Au and Pt on poly(taurine)/GCE obtained from EDX data were 23.24 and 11.77, respectively (Figure 2d,e).

The AFM images of the metal nanoparticles and poly(taurine) film on the ITO were taken to obtain detailed information about the surface morphology and homogeneity of the deposited film at the tapping mode. As seen in Figure 3, a lot of small protuberant peaks were observed in 2D and 3D AFM images of the poly(taurine) surface layer. From the images (Figure 3g and h, AuNPs, and PtNPs) were deposited on the surfaces of poly(taurine)/ITO. The changes in the surface morphology are clearly seen from the figures.



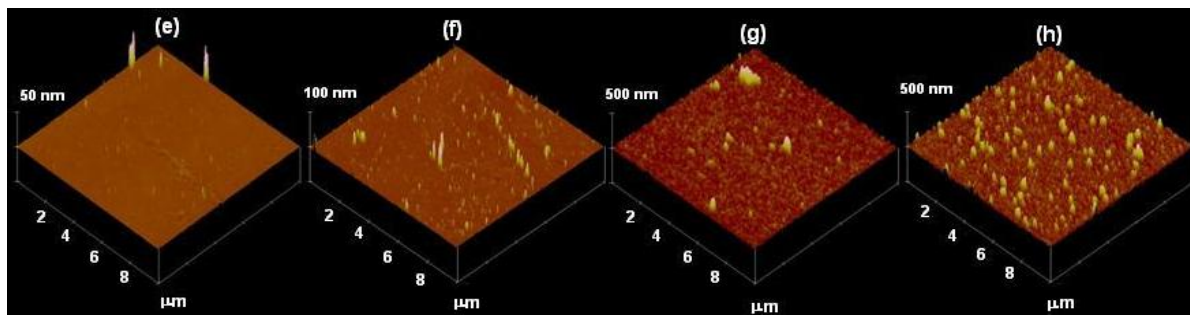


**Figure 3.** AFM images of (a) Bare ITO, (b) poly(taurine)/ITO, (c) AuNPs/poly(taurine)/ITO, (d) PtNPs/poly(taurine)/ITO (2D) and 3D (e) Bare ITO, (f) poly(taurine)/ITO, (g) AuNPs/poly(taurine)/ITO, (h) PtNPs/poly(taurine)/ITO.

The root-mean-square (rms) roughness of bare ITO, poly(taurine), AuNPs/poly(taurine), and PtNPs/poly(taurine) were calculated as 1.003 nm, 2.413 nm, 18.973 nm, and 27.686 nm, respectively (Table 1). Figure 3D-h indicate homogeneous surface properties and existence of Pt nanoparticles on well covered by poly(taurine). These AFM images agree substantially with previous studies [36, 37].

**Table 1.** Values of selected roughness parameters measured from the surface analysis of AFM topography images for ITO and modified ITO.

Electrodes	Roughness Average (Ra) (nm)	Root mean square (RMS) roughness (nm)
Bare ITO	1.003	18.1
poly(taurine)/ITO	2.413	34.2
AuNPs/poly(taurine)/ITO	18.973	28.4
PtNPs/poly(taurine)/ITO	27.686	31.6

X-ray diffraction (XRD) was used widely to analyze the configuration of materials and their crystallographic structures. The samples were scanned from 20 to 70 2Theta in step sizes of 0.0130. To phase identification, the contents of samples were used in the HighScore database program. The XRD patterns of PtNPs/poly(taurine) and AuNPs/poly(taurine) on the indium tin oxide (ITO) glass were analysed (Figure 4). The strong and sharp diffraction peaks indicated that ITO were highly crystalline. The XRD pattern peaks matched well with the cubic structure of ITO. The peaks appearing in the XRD patterns agreed with that of the  $\text{In}_2\text{O}_3$  cubic structure [38].

In the XRD pattern in Figure 4, for Pt, the characteristic peak is determined at  $2\theta=39.755^\circ$  intensities and the diffraction peak at  $2\theta=39.755^\circ$  was observed, which correspond to the (111) crystalline planes of face-centered cubic Pt crystal. For gold, the characteristic 100% peak is determined at  $2\theta=38.18^\circ$  intensities, corresponding to the (111), which is the index of a face-centered cubic of Au. These data agree substantially with previous studies [39]. Au and Pt nanoparticles on the poly(taurine) surface were confirmed as pure metal nanoparticles by XRD analysis.

The electrochemical impedance spectroscopy (EIS) was an effective technique to investigate the electron-transfer properties of the modified surfaces and it is often used for understanding chemical transformations. Figure 5 shows the Nyquist plot of bare GCE, poly(aurine)/GCE, AuNPs/poly(aurine)/GCE, and PtNPs/poly(aurine)/GCE in the presence of 5.0 mM ferri/ferrocyanide  $[\text{Fe}(\text{CN})_6]^{3-/4-}$  containing 0.1 M KCl solution at a frequency range of 0.05 to 30.000 Hz. The Nyquist plot includes a semicircle portion at higher frequencies corresponding to the electron transfer-limited process and a linear part at lower frequency range, representing the diffusion-limited process. The semicircle diameter in the Nyquist plot infers the charge transfer resistance ( $R_{ct}$ ).

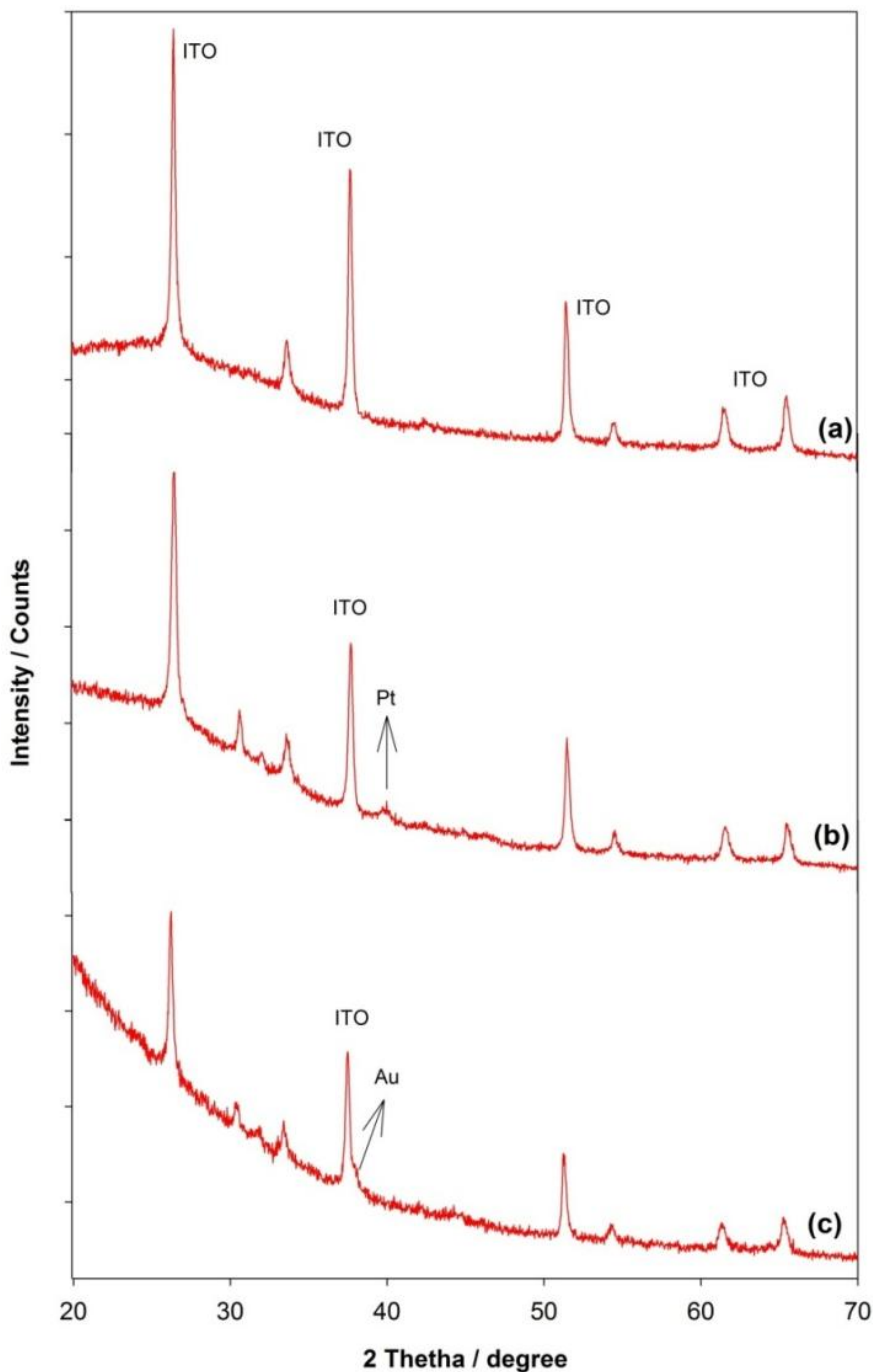


**Figure 4.** XRD pattern of a) Bare ITO, b) PtNPs/poly(aurine)/ITO, c) AuNPs/poly(aurine)/ITO

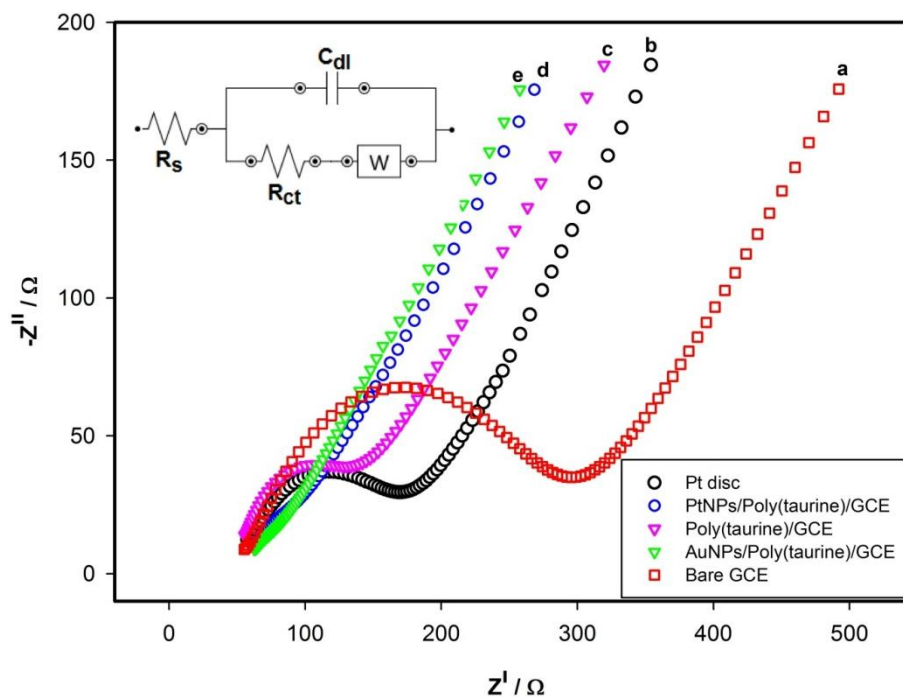


**Figure 5.** Nyquist plots for (a) Pt disc, (b) bare GCE, (c) AuNPs/poly(aurine)/GCE (d) poly(aurine)/GCE and (e) PtNPs/poly(aurine)/GCE in 5mM  $K_3[Fe(CN)_6]/K_4[Fe(CN)_6]$  (1:1) containing 0.1 M KCl with frequency of 0.05 Hz – 30,000 Hz

The EIS data were fitted with an  $R(C(R_{ct}W))$  equivalent circuit. A large semicircle was obtained as a high electron transfer resistance (250 ohm) in the bare GC electrode compared to the other electrodes. The  $R_{ct}$  value of Pt disc (140 ohm) was higher compared to poly(aurine)/GCE. On the other hand, poly(aurine)/GCE had a 80-ohm  $R_{ct}$  value that was lower than bare GCE. The smaller  $R_{ct}$  value confirmed the good conductivity observed for PtNPs/poly(aurine)/GCE (50 ohm) and AuNPs/poly(aurine)/GCE (35 ohm). The good conductivity of the metal modified electrodes may be attributed to the synergistic effect of Pt and Au nanoparticles with the conducting polymer, which can greatly improve the electron transfer rate. This clearly improved the excellent electro conductivity, which was proved by PtNPs/poly(aurine)/GCE surface.

### 3.2. Optimization Studies for Hydrazine

The scan number of polymerization was an important parameter to control the film thickness on the modified electrode surface. The effect of scan numbers of poly(aurine) on the peak current of hydrazine on GCE was investigated with cyclic voltammetry. As seen in Figure 6, the peak current increased with the increasing number of cyclic voltammetric scans. The current response was increase up to scan number of 10 and decreases thereafter. Thus, we chose 10 cycles as the optimum scan number for poly(aurine) in this study. In the same way, the scan numbers of Au and Pt nanoparticles were optimized and maximum current response was obtained at scan number of 8.

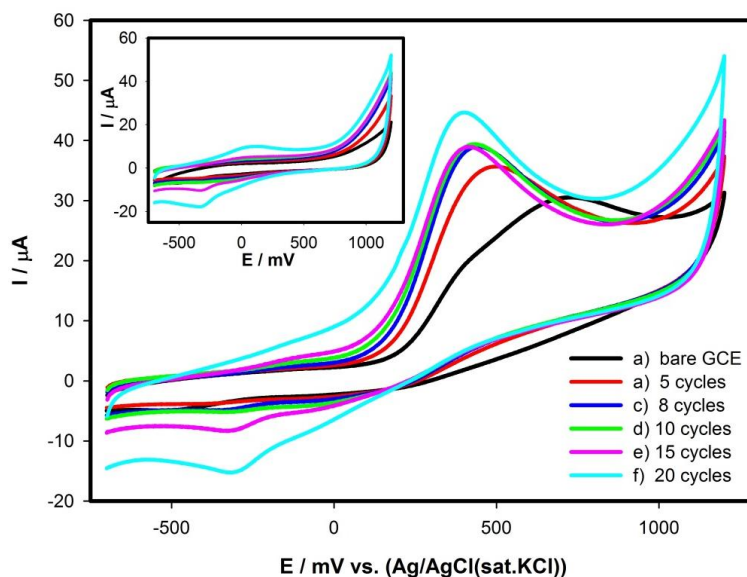


**Figure 6.** Cyclic voltammograms of 1.0 mM hydrazine at the electrode modified different cycles number of taurine on the GCE in 0.1 M pH 7.0 PBS, Scan rate:  $50 \text{ mV s}^{-1}$ . Inset: voltammograms of background for electrodes in pH 7.0 PBS.

### 3.3. Comparison of the modified electrodes

To understand the electrocatalytic activity of modified electrodes towards hydrazine oxidation, bare and modified electrodes were studied with linear sweep voltammetry in a pH 7.0 PBS. Figure 7 shows the voltammograms of hydrazine at the bare GCE, poly(taurine)/GCE, AuNPs/poly(taurine)/GCE, and PtNPs/poly(taurine)/GCE. Bare GCE exhibited poor current response ( $690 \text{ mV}$ ,  $18.1 \mu\text{A}$ ) towards hydrazine oxidation. The hydrazine oxidation signal was improved by the modification of GCE with poly(taurine). The oxidation peak was observed at  $401 \text{ mV}$  with  $31.6 \mu\text{A}$  current value in the presence of poly(taurine) film. Pt and Au disc electrodes were also used in order to compare the real effect of metal nanoparticles on hydrazine oxidation.

Hydrazine oxidation was obtained at  $403 \text{ mV}$  with  $33.2 \mu\text{A}$  at Au disc electrode while a negative potential ( $341 \text{ mV}$  with  $58.0 \mu\text{A}$ ) was observed at AuNPs/poly(taurine)/GCE electrode. Hydrazine oxidation peak potential was shifted about  $300 \text{ mV}$  in negative direction with about 2.0 times higher peak current value as compared to the bare GCE. Moreover, hydrazine oxidation was obtained at  $-280 \text{ mV}$  with  $28.4 \mu\text{A}$  at Pt disc electrode while more negative peak potential ( $-370 \text{ mV}$  with  $45.5 \mu\text{A}$ ) was observed at PtNPs/poly(taurine)/GCE electrode. The background voltammograms of all electrodes were shown in inset of Figure 7. The best catalytic activity in terms of peak potential was obtained with Pt nanoparticles on poly(taurine)/GCE electrode with a  $1060 \text{ mV}$  potential shift to negative and about 3 times higher peak current as compared to the bare GCE. These results showed that metal nanoparticles deposition catalyses the oxidation process in terms of both potential shift to negative values and current increase as compared to the disc electrodes and metal nanoparticle modified surfaces. The comparisons revealed that the Au nanoparticles have much stronger catalytic activity toward the oxidation of hydrazine than Pt nanoparticles on the poly(taurine) modified glassy carbon electrode. These results showed that the electrocatalytic activity of modified

electrodes towards hydrazine oxidation was increased due to the interaction of Au and Pt nanoparticles with the functional groups on the surface of poly(aurine)such as  $-NH_2$ ,  $-SO_2$ , and  $-OH$ .

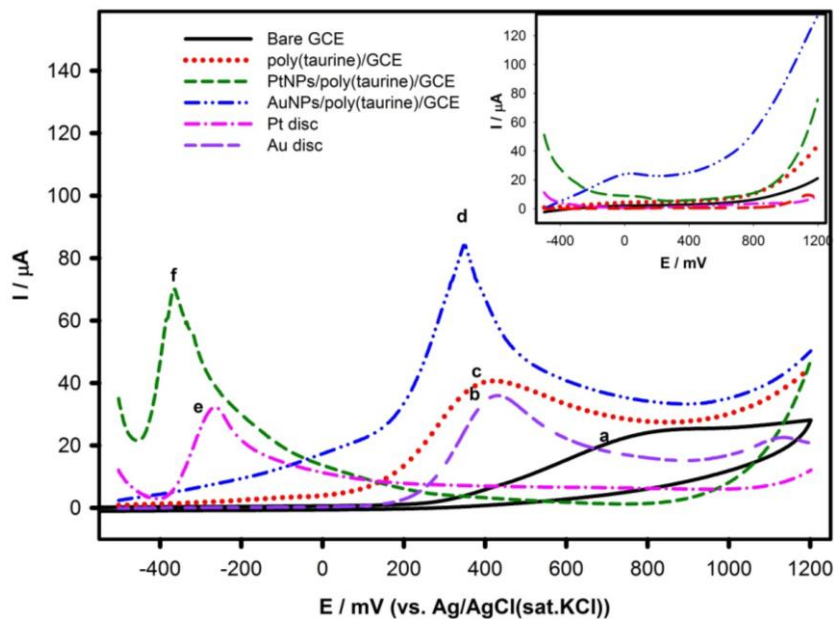


**Figure 7.** Linear sweep voltammograms of 1 mM hydrazine in pH 7.0 PBS, (a) Bare GCE, (b) Au disc, (c) poly(aurine)/GCE, (d) AuNPs/poly(aurine)/GCE, (e) PtNPs/poly(aurine)/GCE, (f) Pt disc, Scan rate:  $50 \text{ mV s}^{-1}$ . Insets: voltammograms of background for all electrodes in pH 7.0 PBS.

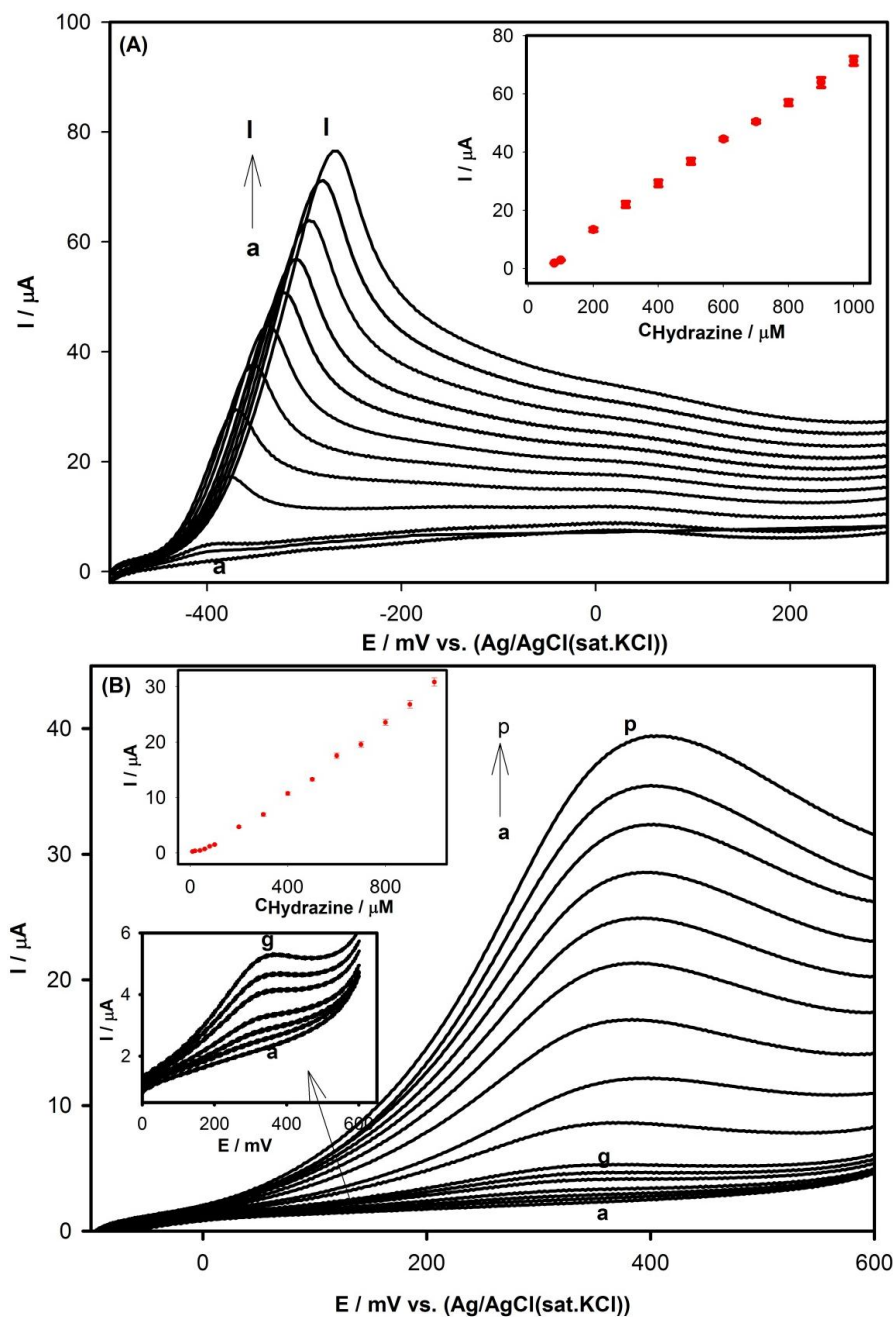
**Table 2.** Characteristics of the peak current and potential for 1.0 mM hydrazine at bare and modified electrodes

Electrode	E (mV)	I ( $\mu\text{A}$ )
GCE	690	18.1
Au disc	403	34.2
Pt disc	-280	28.4
poly(aurine)/GCE	401	31.6
AuNPs/poly(aurine)/GCE	341	58.0
PtNPs/poly(aurine)/GCE	-370	45.5

### 3.4. Determination of hydrazine

LSV and amperometric methods were used for the comparison of the analytical performance of the PtNPs/poly(aurine)/GCE and AuNPs/poly(aurine)/GCE towards hydrazine determination. Figure 8 shows the typical LSV of hydrazine oxidation at Au and PtNPs modified electrodes for increasing concentrations of hydrazine in  $N_2$  saturated 0.1 M pH 7.0 PBS. In Figure 8A and inset show the increasing concentrations of hydrazine and related calibration graph that were obtained at PtNPs/poly(aurine)/GCE. The current increase were found linear in the concentration range of 80 to 1000  $\mu\text{M}$ . The linear regression equation is:  $i(\mu\text{A}) = 0.0748 C(\mu\text{M}) - 1.9997$ , with correlation

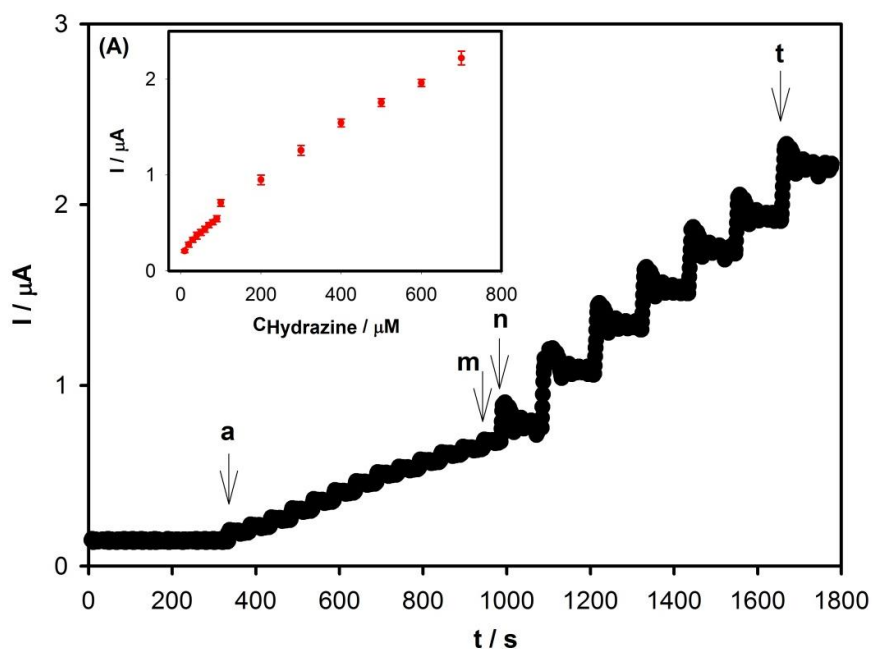
coefficients of 0.9956. The limit of detection was found to be 36  $\mu\text{M}$ . Also, Figure 8B shows LSVs of increasing hydrazine concentrations at AuNPs/poly(aurine)/GCE that found linear in the range of 0.1 to 1000  $\mu\text{M}$ . The linear regression equation is:  $i(\mu\text{A}) = 0.0308 C(\mu\text{M}) - 1.1664$ , with correlation coefficients of 0.9981. The limit of detection was calculated to be 5  $\mu\text{M}$ . Figures show that more sensitive results for hydrazine detection was obtained at AuNPs/poly(aurine)/GC electrode as compared to the PtNPs/poly(aurine)/GC electrode.



**Figure 8.** Linear sweep voltammograms of different hydrazine concentrations at PtNPs/poly(aurine)/GCE (A) (a) 0.1 M pH 7.0 PBS, (b) 80, (c)100, (d) 200, (e) 300, (f)400, (g) 500, (h) 600, (i) 700, (j) 800, (k) 900, (l) 1000  $\mu\text{M}$ , and at AuNPs/poly(aurine)/GCE (B), (a) 0.1 M pH 7.0 PBS, (b) 10, (c) 20, (d) 40, (e) 60, (f) 80, (g) 100, (h) 200, (i) 300, (j) 400, (k) 500, (l) 600, (m) 700, (n) 800, (o) 900, (p) 1000  $\mu\text{M}$ .

Amperometric methods are often used for the hydrazine sensors. Figure 9A shows the typical amperometric current–time (i-t) response on AuNPs/poly(aurine)/GC electrode for increasing hydrazine concentration into a stirred solution of 0.1 M pH 7.0 PBS at an applied potential at 0.4 V. It can be seen that the amperometric current increases obviously after each injection of hydrazine and the chronoamperometric responses achieved a steady-state signal within 20 s. The inset of Figure 9A represents the calibration graphs of the response currents versus hydrazine concentration. The current increases were found linear in the concentration range of 0.1 to 1000  $\mu\text{M}$ . The linear regression equation is:  $I(\mu\text{A}) = 0.0029 C(\mu\text{M}) - 0.2803$ , with a 0.9981 correlation coefficient. The limit of detection (LOD) and the limit of quantification (LOQ) values were calculated to be 0.05  $\mu\text{M}$  and 0.15  $\mu\text{M}$ , respectively. The LOD and the LOQ were calculated using the formula  $\text{LOD}=3.3 \text{ SD}/b$  and  $\text{LOQ}=10 \text{ SD}/b$ , respectively, where SD is the standard deviation of five reagent blank determinations and b is the slope of the calibration curve. This result suggested that the high ability of AuNPs/poly(aurine)/GCE as an electrochemical sensor for the sensitive detection of hydrazine. The comparison between previously reported chemically modified electrodes for the determination of hydrazine is listed in Table 3.

The selectivity of the proposed sensor toward hydrazine detection was investigated in the presence of a various interferences such as  $\text{Cd}^{2+}$ ,  $\text{Pb}^{2+}$ ,  $\text{Zn}^{2+}$ ,  $\text{Cu}^{2+}$ ,  $\text{NO}_3^-$ ,  $\text{Cl}^-$ , and  $\text{SO}_4^{2-}$  (Figure 9B). The interference study was performed on the AuNPs/poly(aurine)/GCE sensor that change in the amperometric hydrazine response was monitored in 0.1 M pH 7.0 PBS solution at an applied potential of 0.400 V. AuNPs/poly(aurine)/GCE sensor exhibited well defined response toward each; a) 20, b) 50, c) 80, and d) 100  $\mu\text{M}$  hydrazine, whereas no remarkable effect was observed for 50 fold excess concentration of  $\text{Cd}^{2+}$ ,  $\text{Pb}^{2+}$ ,  $\text{Zn}^{2+}$ ,  $\text{Cu}^{2+}$ ,  $\text{SO}_4^{2-}$  and in the presence of 100 folds excess concentrations of  $\text{NO}_3^-$  and  $\text{Cl}^-$ . These results indicated that the AuNPs/poly(aurine)/GCE was highly selective electrode towards the detection of hydrazine. This electrode was useful for the determination of hydrazine in the real samples without any interference.



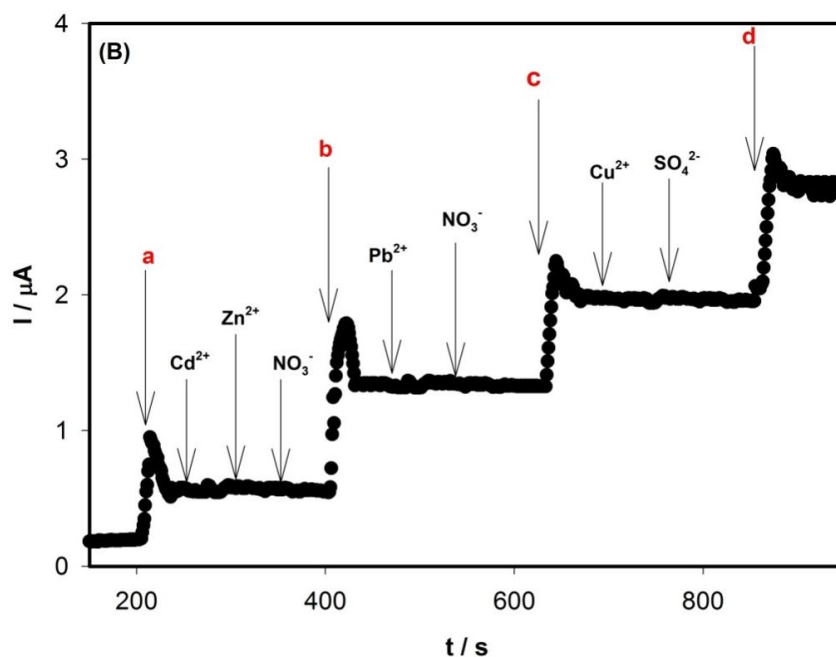


**Figure 9.** A) Amperometric  $i-t$  response of AuNPs/poly(taurine)/GCE by stepwise addition at different concentrations of hydrazine into the stirring  $N_2$ -saturated 0.1 M pH 7.0 PBS at an applied potential of 0.4 V. Inset: calibration curve of hydrazine current response versus its concentration. B) Amperometric response of AuNPs/poly(taurine)/GCE for the successive injection of at different concentrations of (a) 20, (b) 50, (c) 80 and (d) 100  $\mu\text{M}$  hydrazine, in presence of 50 fold excess concentration of ascorbic acid (AA),  $\text{Cd}^{2+}$ ,  $\text{Pb}^{2+}$ ,  $\text{Zn}^{2+}$ ,  $\text{Cu}^{2+}$ ,  $\text{SO}_4^{2-}$ , and in the presence of 100 folds excess concentrations of  $\text{NO}_3^-$ ,  $\text{Cl}^-$ .

**Table 3.** Comparison of the performance of the proposed hydrazine sensor with previously reported electrodes for hydrazine detection.

Electrode	Methods	Medium	Linear range ( $\mu\text{M}$ )	Detection limit ( $\mu\text{M}$ )	Ref.
Au/PPy/GCE	DPV	PBS	1–7500	0.2	[12]
ZnO nanonails	Amperometry	PBS	0.1–1.2	0.2	[1]
Ni/BA–MWCNT/PE	Amperometry	NaOH	2.5–200	0.8	[14]
Pd/PANI–PAMPSA	Amperometry	PBS	40–1000	0.4	[31]
QLO@MWCNT/GCE	Amperometry	PBS	25–450	12	[40]
AuNPs/poly(BCP)/CNT/GCE	LSV	PBS	0.5–1000	0.1	[5]
PtNPs/poly(BCP)/CNT/GCE	LSV	PBS	20–800	2	[34]
PtNPs/poly(taurine)/GCE	LSV	PBS	80–1000	36	This work
AuNPs/poly(taurine)/GCE	LSV	PBS	0.1–1000	5	This work
AuNPs/poly(taurine)/GCE	Amperometry	PBS	0.1–1000	0.05	This work

(DPV) differential pulse voltammetry; (LSV) linear sweep voltammetry. Au/PPy/GCE, gold and polypyrrole modified glassy carbon electrode, Ni(II)/BA–MWCNT-PE, nickel(II)–baicalein

complex on the multiwall carbon nanotube paste electrode; Pd/PANI–PAMPSA, Poly(2-acrylamido-2-methyl-propane-sulfonic acid)-doped polyaniline Pd nanoparticles; QLO@MWCNT/GCE, quinoline quinones on MWCNT modified glassy carbon electrode; MWCNT, multiwalled carbon nanotubes; PE, paste electrode; NPs, nanoparticles; PBS, phosphate buffer solution.

### 3.5. Real sample analysis

The AuNPs/poly(aurine)/GCE electrode was applied to determination of hydrazine in Gediz river water. The samples were analyzed by amperometry. For the analysis, 3.0 mL of the river water was diluted to 10 mL with 0.1 M pH 7.0 PBS. The results are summarized in Table 4. The hydrazine in the Gediz river samples was not detected. Also, for the recoveries, the standard concentrations of hydrazine (1, 100 and 500  $\mu\text{M}$ ) were spiked in the river sample and analyzed using the amperometric method ( $n=4$ ). The results showed that the recoveries were obtained ranged between 99%-104%. The significant recoveries were achieved for the determination of trace level of hydrazine in the Gediz river samples.

**Table 4.** Recovery analysis of hydrazine determination in real samples at AuNPs/poly(aurine)/GCE.

Sample	Modified electrode			
	AuNPs/poly(aurine)/GCE			
	Added ( $\mu\text{M}$ )	Detected ( $\mu\text{M}$ )	Recovery (%)	Relative standard deviation ( $n=4$ )
Gediz River	0.00	0.00	-	-
	1.00	1.04	104.0	2.2
	100.00	98.80	98.8	1.5
	500.00	515.00	103.0	2.1

### 3.6. The stability and reproducibility

The stability and durability of catalysts are also an important parameter for sensor application that studied on AuNPs/poly(aurine)/GCE and PtNPs/poly(aurine)/GCE. The stability of the four different electrodes was examined. The chronoamperometric curves of different electrode potentials are shown in Figure 10. The curves of bare and modified electrodes were also tested for comparison. The chronopotentiograms were recorded by holding the constant oxidation potential of hydrazine at each electrode for 600 s. At AuNPs/poly(aurine)/GC electrode, the current densities reached a steady-state after a few seconds and displayed no decrease within a test period, and AuNPs/poly(aurine)/GCE modified electrode has superior stability. Compared to the AuNPs/poly(aurine)/GCE and PtNPs/poly(aurine)/GCE catalysts, the AuNPs/poly(aurine)/GCE catalysts had a better stability in 1.0 mM hydrazine. However, current densities of the bare electrode and poly(aurine)/GCE lower than other modified electrodes which reach steady-state within a 600 s test period. Obviously, it can be found that at the absolute current density on an AuNPs/poly(aurine)/GCE electrode, it is significantly larger than that of the other electrodes.

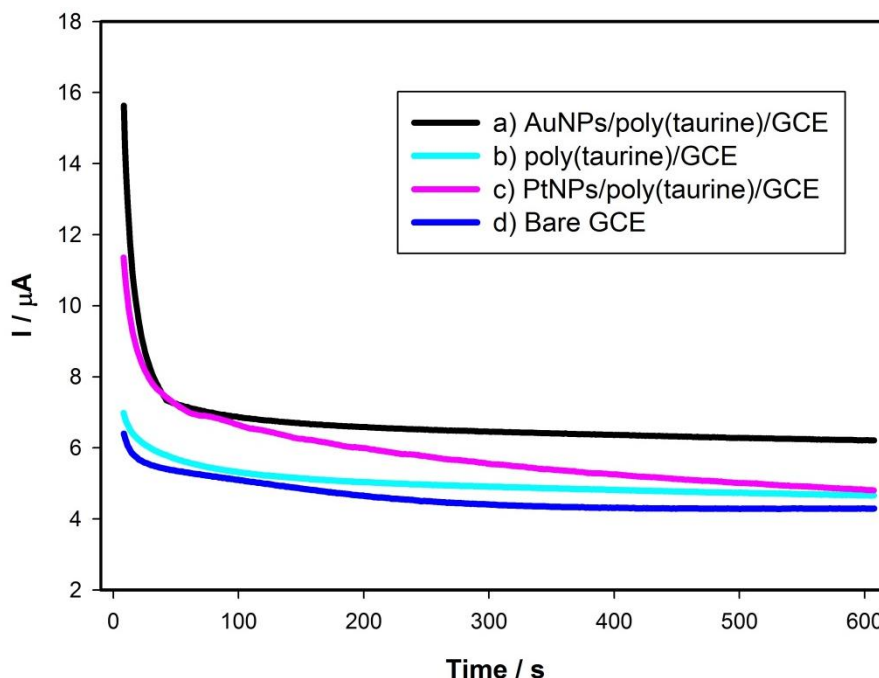


**Figure 10.** Chronoamperograms of bare and modified electrodes in pH 7.4 PBS containing 1.0 mM hydrazine.

The stability and repeatability of AuNPs/poly(aurine)/GCE and PtNPs/poly(aurine)/GCE electrodes toward the hydrazine oxidation reaction were also tested by using cyclic voltammetric measurement for a period of three weeks. The storage stability of the modified electrodes were verified by measuring the oxidation currents in solutions in the presence of 1.0 mM hydrazine in 0.1 M pH 7.0 PBS. AuNPs/poly(aurine)/GC and PtNPs/poly(aurine)/GC electrodes were stored in 0.1 M pH 7.0 PBS in at room temperature. There was no significant peak potential shift observed for hydrazine oxidation that the current signals showed less than a 2.0% decrease relative to the initial response.

The generation of reproducible electrode surface was examined by using cyclic voltammetry data from six modified electrodes. The relative standard deviation (RSD) obtained, was lower than 2.3% for the peak current of hydrazine at different modified electrodes. These results indicated that metal nanoparticle modified electrodes has good stability and reproducibility.

#### 4. CONCLUSION

In this work, poly(aurine)/GCE, AuNPs/poly(aurine)/GCE, and PtNPs/poly(aurine)/GCE were simply prepared and used for the oxidation of hydrazine in neutral pH by cyclic voltammetry technique. The oxidation peak current of hydrazine in the AuNPs/poly(aurine)/GCE and PtNPs/poly(aurine)/GCE were increased significantly. This behavior can be attributed to the synergistic effect of metal nanoparticles and poly(aurine) film. The interaction of Au and Pt nanoparticles with the functional groups, such as  $-NH_2$ ,  $-SO_2$ , and  $-OH$  in the structure of poly(aurine) revealed a higher electrocatalytic catalytic activity towards hydrazine oxidation. The modified electrodes had good stability, sensitivity, and selectivity. The proposed method has also been successfully and practically applied for the determination of hydrazine.

## References

1. A. Umar, M.M. Rahman, S.H. Kim and Y.B. Hahn, *Chem. Commun.*, 2 (2008) 166.
2. S.M. Golabi and H.R. Zare, *J. Electroanal. Chem.*, 465 (1999) 168.
3. A. Safavi, F. Abbasitabar and M.R. Hormozi Nezhad, *Chem. Anal. (Warsaw)*, 52 (2007) 835.
4. D. Jayasri and S.S. Narayanan, *J. Hazard. Mater.*, 144 (2007) 348.
5. S. Koçak and B. Aslışen, *Sens. Actuators B*, 196 (2014) 610.
6. J.S. Budkuley, *Mikrochim. Acta*, 108 (1992) 103.
7. A. Safavi and M.A. Karimi, *Talanta*, 58 (2002) 785.
8. M. Ebadi, *Can. J. Chem.*, 81 (2003) 161.
9. R. Gilbert, R. Rioux and S.E. Saheb, *Anal. Chem.*, 56 (1984) 106.
10. L. Zheng and J.F. Song, *Sens. Actuators B*, 135 (2009) 650.
11. K.I. Ozoemena, T. Nyokong, *Talanta*, 67 (2005) 162.
12. J. Li and X. Lin, *Sens. Actuators B*, 126 (2007) 527.
13. H.J. Zhang, J.S. Huang, H.Q. Hou and T.Y. You, *Electroanalysis*, 21 (2009) 1869.
14. L. Zheng and J.F. Song, *Talanta*, 79 (2009) 319.
15. A. Salimi, L. Miranzadeh and R. Hallaj, *Talanta*, 75 (2008) 147.
16. Y. Wang and Z. Z. Chen, *Colloids Surf. B*, 74 (2009) 322.
17. Q. Wan, X. Wang, F. Yu, X. Wang and N. Yang, *J. Appl. Electrochem.*, 39 (2009) 785.
18. X.Q. Xiong, K.J. Huang, C.X. Xu, C.X. Jin and Q.G. Zhai, *Chem. Ind. Chem. Eng. Q.*, 19 (2013) 359.
19. M. Rajkumar, Y.S. Li and S.M. Chen, *Colloids Surf. B*, 110 (2013) 242.
20. C.W. Welch and R.G. Compton, *Anal. Bioanal. Chem.*, 384 (2006) 601.
21. K. Cui, Y.H. Song, Y. Yao, Z.Z. Huang and L. Wang, *Electrochem. Commun.*, 10 (2008) 663.
22. R. Narayanan and M.A. El-sayed, *J. Phys. Chem. B*, 109 (2005) 12663.
23. X. Li, J. Sun and M. Huang, *Progr. Chem.*, 19 (2007) 787.
24. J. Pillay, K.I. Ozoemena, R.T. Tshikhudo, and R.M. Moutloali, *Langmuir*, 26 (2010) 9061.
25. J. Li, H. Xie and L. Chen, *Sens. Actuators B*, 153 (2011) 239.
26. M. A. Aziz and A.N. Kawde, *Talanta*, 115 (2013) 214.
27. S. Koçak, A. Altın and Ç.C. Koçak, *Anal. Lett.*, xx (2016) xx  
DOI:10.1080/00032719.2015.1045586 (in press).
28. J. Kasthuri and N. Rajendiran, *Colloids Surf. B*, 73 (2009) 387.
29. P. Paulraj, N. Janaki, S. Sandhya and K. Pandian, *Colloids Surf. A*, 377 (2011) 28.
30. Q. Yi, F. Niu and W. Yu, *Thin Solid Films*, 519 (2011) 3155.
31. V. Lyutov and V. Tsakova, *J. Electroanal. Chem.*, 661 (2011) 186.
32. S. Ivanov, U. Lange, V. Tsakova and V.M. Mirsky, *Sens. Actuators B*, 150 (2010) 271.
33. S. Chakraborty and C.R. Raj, *Sens. Actuators B*, 147 (2010) 222.
34. S. Koçak, B. Aslışen and Ç.C. Koçak, *Anal. Lett.*, xx (2016) xx  
DOI:10.1080/00032719.2015.1038548 (in press).
35. H. Song, Y. Ni and S. Kokot, *Anal. Chimica Acta*, 788 (2013) 24.
36. V.C. Ferreira, A.I. Melato, A.F. Silva and L.M. Abrantes, *Electrochim. Acta*, 56 (2011) 3567.
37. H. Chen and S. Dong, *Talanta*, 71 (2007) 1752.
38. S.R. Ramanan, *Thin Solid Films*, 389 (2001) 207.
39. V. Vinoth, J.J. Wu, A.M. Asiri and S. Anandan, *Sens. Actuators B*, 210 (2015) 731.
40. P. Swetha, K.S.S. Devi and A.S. Kumar, *Electrochim. Acta*, 147 (2014) 62.